Recent work on time-frequency representation and compressive sensing

Xiumei Li, Hangzhou Normal University

2 August, 2015

Outline

- Work on time-frequency representation (TFR)
- Work on compressive sensing
- Work on compressive sensing based TFR
- Future work

Outline

- Work on time-frequency representation (TFR)
  - Introduction
  - Local polynomial Fourier transform (LPFT)
- Work on compressive sensing
- Work on compressive sensing based TFR
- Future work

Introduction, Cont'd

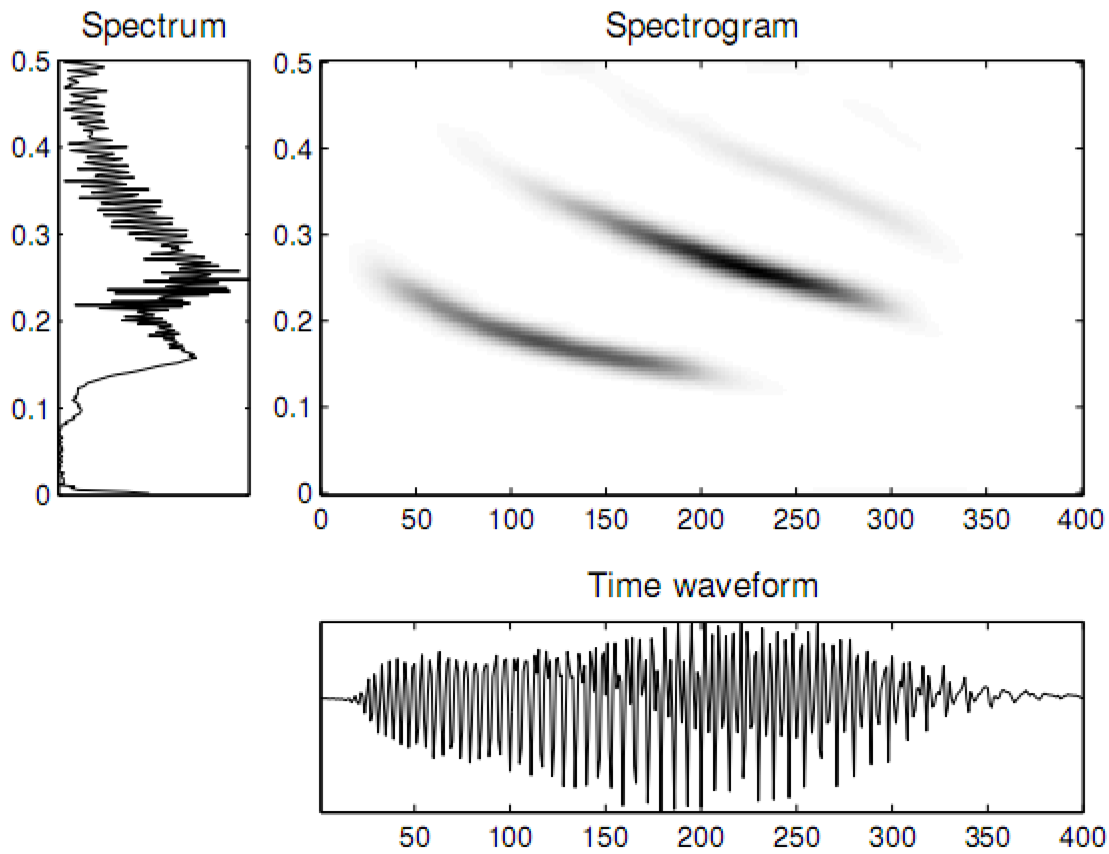

The time waveform, spectrum, and time-frequency representation (TFR) of the bat sound data.

Introduction, Cont'd

- Although there are many different TFRs, such as the short-time Fourier transform (STFT) and Wigner-Ville distribution (WVD), each has its individual limits.
  - The STFT assumes that the frequency of the signal within a segment is not changing with time, its resolution for time-varying signal is rather low.
  - WVD suffers from the cross-term for multi-component signals.

- The local polynomial Fourier transform (LPFT) is used to overcome these limits [V. Katkovnik, Signal Processing, 1995]
  - The LPFT is a linear transform, thus is free from the cross-term.
  - The LPFT can provide high resolution for time-varying signals with a local polynomial function approximating to the instantaneous frequency (IF) characteristic of the analyzed signals.
  - Disadvantage: heavy computational load (reduced overlap, various fast algorithms)

Outline

- Work on time-frequency representation (TFR)
  - Introduction
  - Local polynomial Fourier transform (LPFT)
    - Definition
    - Uncertainty principles of second-order and higher-order LPFT
    - Reassignment method for second-order and higher-order LPP
- Work on compressive sensing
- Work on compressive sensing based TFR
- Future work

LPP: local polynomial periodogram

Local polynomial Fourier transform

- The LPFT, the generalized form of the STFT, is defined as [V. Katkovnik, Signal Processing, 1995]

$$LPFT(t,\varpi) = LPFT(t,\omega,\omega_1,\ldots,\omega_{M-1})$$
$$= \int x(t+\tau)h^*(\tau)e^{-j\theta(\tau,\varpi)}d\tau$$

where

$$\theta(\tau,\varpi) = \omega\tau + \omega_1\tau^2/2 + \ldots + \omega_{M-1}\tau^M/M!$$
$$\varpi = (\omega,\omega_1,\ldots,\omega_{M-1})$$

M: the order of the LPFT

- LPFT assumes that the frequency of the signal within a segment is changing with time.

Local polynomial Fourier transform, Cont'd

- The polynomial time frequency transform (PTFT) is an important tool for the analysis of PPSs. It is the maximum likelihood estimator (MLE) to find the parameters for the PPSs.
- For a PPS, the PTFT yields the same number of peaks as that of components in the PPS.
- The parameters of the LPFT can be estimated from the location coordinates of the peaks.

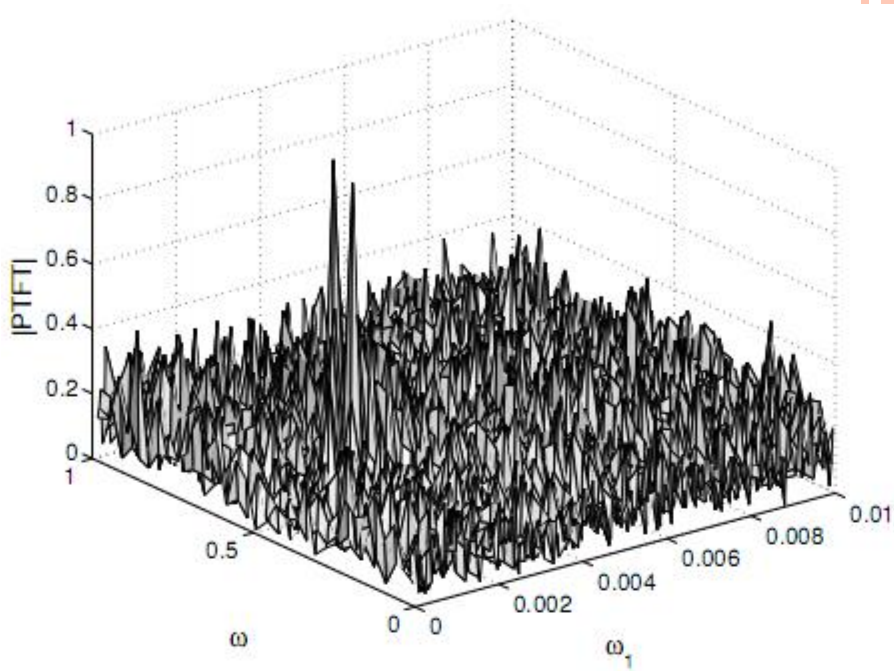

The PTFT of the sum of two second-order PPSs (SNR = 0dB).

Outline

- Work on time-frequency representation (TFR)
  - Introduction
  - Local polynomial Fourier transform (LPFT)
    - Definition
    - Uncertainty principles of second-order and higher-order LPFT
    - Reassignment method for second-order and higher-order LPP
- Work on compressive sensing
- Work on compressive sensing based TFR
- Future work

UNCERTAINTY PRINCIPLE OF THE LPFT

- The LPFT is particularly suited to process the PPSs with a Gaussian amplitude defined by

$$s(t) = (\frac{a}{\pi})^{1/4} \exp\{-\frac{at^2}{2}\} \exp\{j\sum_{m=1}^{P} \frac{a_{m-1}t^m}{m!}\}$$

- We use the Gaussian window function

$$h(t) = (\frac{\alpha}{\pi})^{1/4} \exp\{-\frac{\alpha t^2}{2}\}$$

Uncertainty Principle of the LPFT

- The normalized signal within a short duration at time instant t is defined as [L. Cohen, Time-frequency Analysis, 1995]

$$\eta_t(\tau) = \frac{s(\tau)h(\tau - t)\exp\{j\omega t - j\sum_{m=2}^{M}\frac{\omega_{m-1}(\tau - t)^m}{m!}\}}{\sqrt{\int \left| s(\tau)h(\tau - t)\right|^2 d\tau}}$$

which ensures that for any t

$$\int \left|\eta_t(\tau)\right|^2 d\tau = 1$$

- The Fourier transform of this short duration signal (or the modified signal) $\eta_t(\tau)$ is

$$F_t(\omega) = \frac{1}{\sqrt{2\pi}}\int \eta_t(\tau)\exp\{-j\omega\tau\}d\tau$$

Uncertainty Principle of the LPFT, cont'd

- The mean time for this signal segment is defined as

$$\langle \tau \rangle_t = \int \tau |\eta_t(\tau)|^2 d\tau$$

and the duration is

$$T_t^2 = \int (\tau - \langle \tau \rangle_t)^2 |\eta_t(\tau)|^2 d\tau$$
$$= \langle \tau^2 \rangle - \langle \tau \rangle_t^2$$

where

$$\langle \tau^2 \rangle = \int \tau^2 |\eta_t(\tau)|^2 d\tau$$

- The mean frequency and bandwidth of the signal segment are

$$\langle \omega \rangle_t = \int \omega |F_t(\omega)|^2 d\omega$$
$$= \int \eta_t^*(\tau) \frac{1}{j} \frac{d}{d\tau} \eta_t(\tau) d\tau$$

$$B_t^2 = \int (\omega - \langle \omega \rangle_t)^2 |F_t(\omega)|^2 d\omega$$
$$= \langle \omega^2 \rangle - \langle \omega \rangle_t^2$$

where

$$\langle \omega^2 \rangle = \int \omega^2 |F_t(\omega)|^2 d\omega$$
$$= -\int \eta_t^* \frac{d^2}{d\tau^2} \eta_t(\tau) d\tau$$

Uncertainty Principle of the LPFT, cont'd

For the second-order PPS, we achieve

- the mean time $$\langle \tau \rangle_t = \frac{a}{a+\alpha} t$$
- the duration $$T_t^2 = \frac{1}{2(a+\alpha)}$$
- the mean frequency $$\langle \omega \rangle_t = a_0 + \omega_1 t + \frac{a}{a+\alpha}(a_1 - \omega_1)t$$
- the bandwidth $$B_t^2 = \frac{a+\alpha}{2} + \frac{1}{2}\frac{(a_1-\omega_1)^2}{a+\alpha}$$

Uncertainty Principle of the LPFT, cont'd

- The uncertainty product is

$$B_t T_t = \frac{1}{2}\sqrt{1+\frac{(a_1-\omega_1)^2}{(a+\alpha)^2}}$$

the uncertainty product is time independent when Gaussian window is used.

- When the parameter ω_1 is correctly estimated, that is $\omega_1 = a_1$, the mean frequency becomes

$$\langle\omega\rangle_t = a_0 + a_1 t$$

Instantaneous frequency

- The uncertainty product becomes

$$B_t T_t = \frac{1}{2}$$

Uncertainty Principle of the LPFT, cont'd

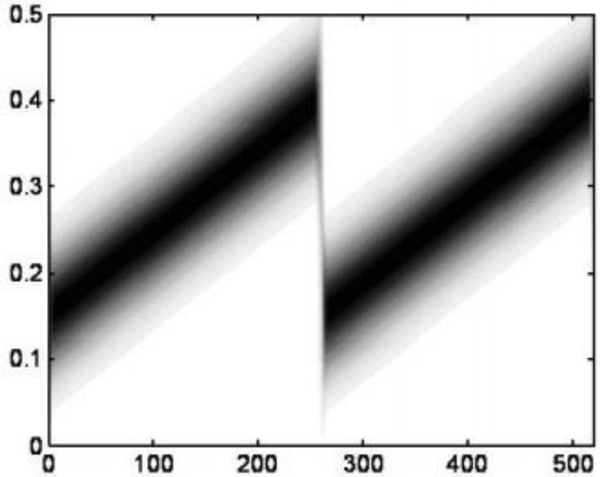

α=50

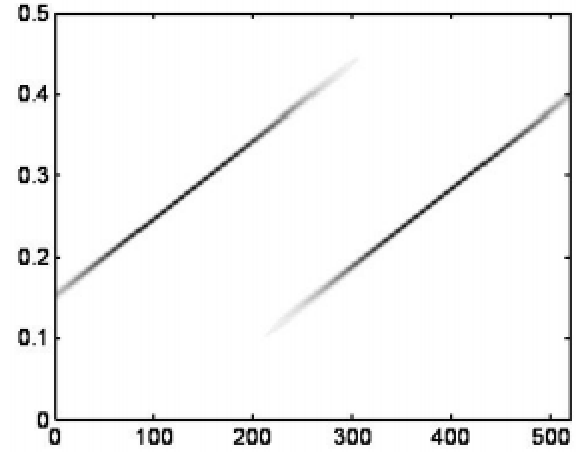

α=2.5

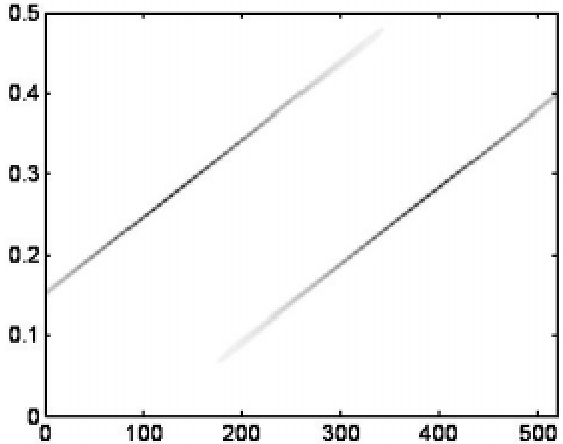

α=0.125

- As α decreases, the resolution of the signal representation in the frequency direction is increased, the resolution in the time direction is decreased.

$$T_t^2 = \frac{1}{2(a+\alpha)}$$

$$B_t^2 = \frac{a+\alpha}{2} + \frac{1}{2}\frac{(a_1-\omega_1)^2}{a+\alpha}$$

Uncertainty principles of the STFT and WVD

- For the STFT of the chirp signal, the mean frequency and bandwidth are

$$\langle \omega \rangle_t = a_0 + \frac{a}{a+\alpha} a_1 t$$

$$B_t^2 = \frac{1}{2}(a+\alpha) + \frac{a_1^2}{2(a+\alpha)}$$

- The WVD of the chirp signal is

$$WVD(t,\omega) = \frac{1}{\pi} \exp\left\{ -at^2 - \frac{(\omega - a_1 t - a_0)^2}{a} \right\}$$

The mean frequency and bandwidth are

$$\langle \omega \rangle_t = a_0 + a_1 t$$

$$B_t^2 = \frac{a}{2}$$

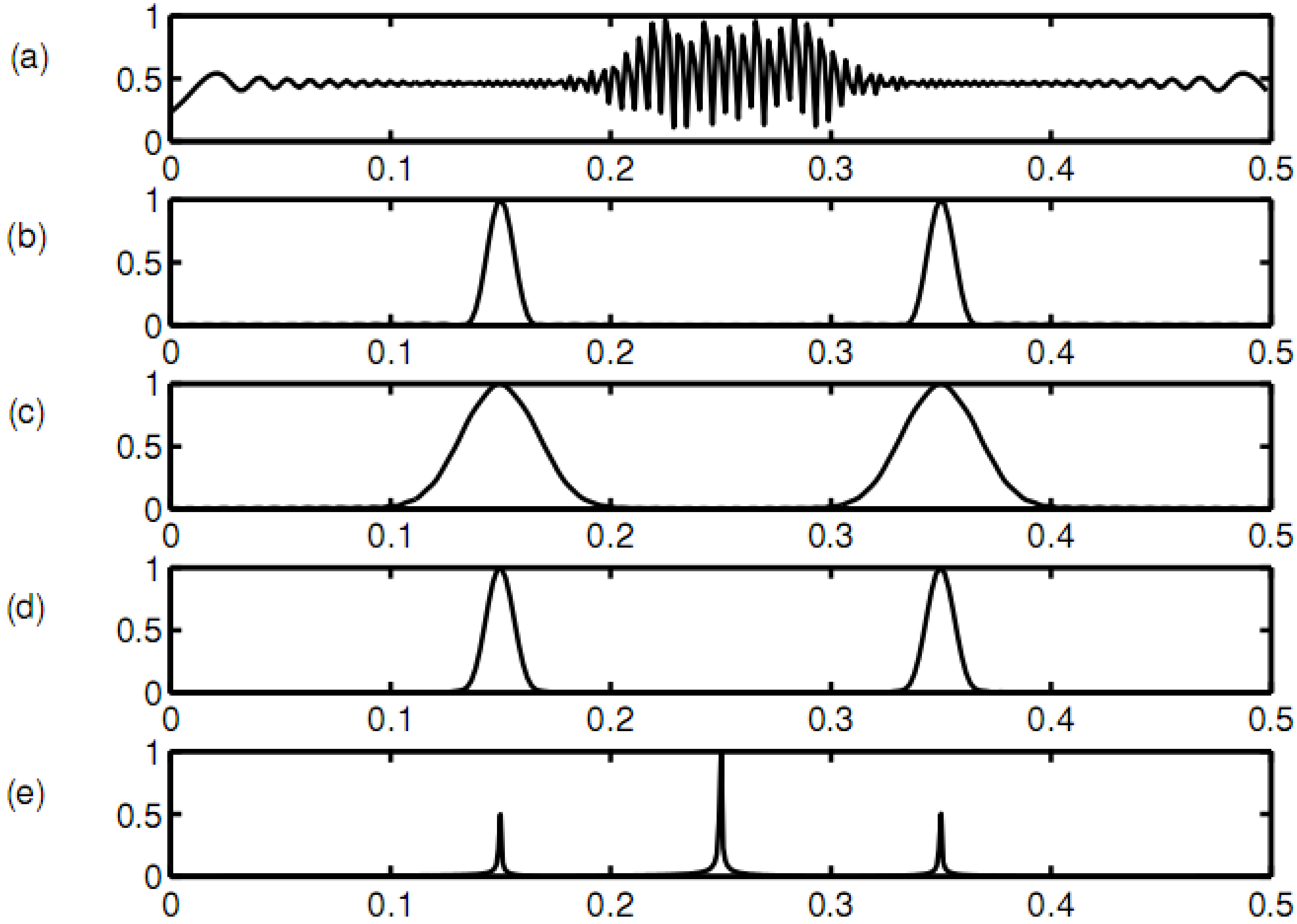

Concentration comparison of the time-frequency representations. (a) the FT of the chirp signals, (b) the STFT of a signal with constant frequencies, (c), (d) and (e) the time-frequency representations of chirp signals using the STFT, the second-order LPFT, and the WVD, respectively.

EXAMPLE: A SPEECH SEGMENT "YOUR MAIL"

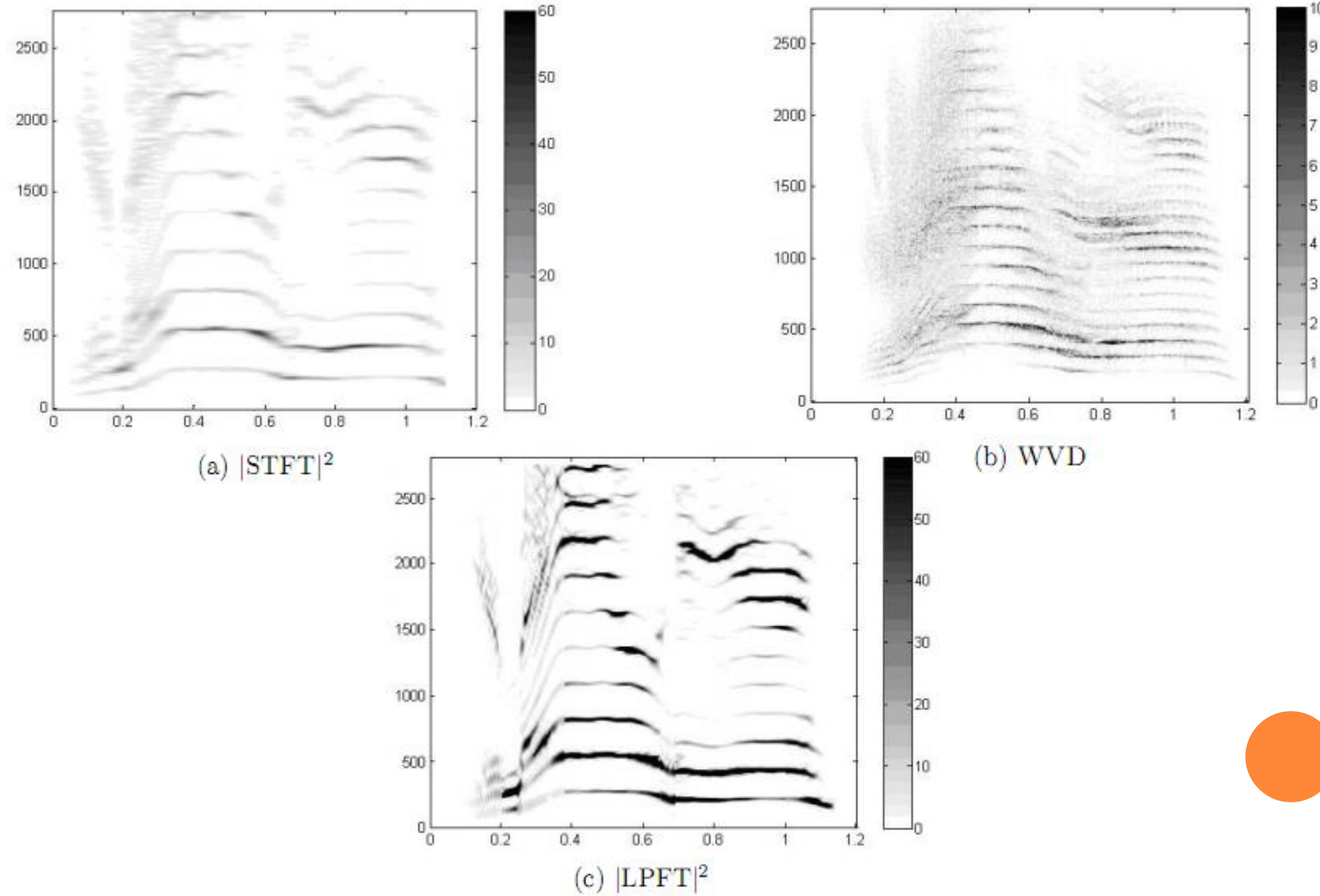

Systematic Analysis of Uncertainty Principles of the LPFT

Table I Expressions of the uncertainty principles for the LPFT

Type of uncertainty principle	Uncertainty product
1. global uncertainty principle	$T_{LPP}^2 B_{LPP}^2 \geq 1$
2. local duration-conditional standard deviation	$\sigma_{\omega\|t}^2 T_t^2 \geq \frac{1}{4}$
3.local bandwidth-conditional standard deviation	$\sigma_{t\|\omega}^2 B_\omega^2 \geq \frac{1}{4}$
4. conditional standard deviations in time and frequency	$\sigma_{t\|\omega}^2 \sigma_{\omega\|t}^2 > \frac{1}{4}$

Table II Expressions of the uncertainty principles for the Mth-order LPFT

Type of uncertainty principle	Uncertainty product
1. global uncertainty principle	$T_{LPP}^2 B_{LPP}^2 \geq 1$
2. local duration-conditional standard deviation	$\sigma_{\omega\|t}^2 T_t^2 \geq \frac{1}{4}$
3.local bandwidth-conditional standard deviation	$\sigma_{t\|\omega}^2 B_\omega^2 \geq \frac{1}{4}$
4. conditional standard deviations in time and frequency	$\sigma_{t\|\omega}^2 \sigma_{\omega\|t}^2 > \frac{1}{4}$

Summary of uncertainty principles of LPFT

- The LPFT is shown to be limited by the uncertainty principle, and the uncertainty principles of various order LPFTs are derived to show the trade-off between the resolutions of signal representation in the time and frequency domains.

- The uncertainty product of an arbitrary order is discussed. When Gaussian window function is employed to segment the signals, the uncertainty products of the LPFT are time independent.

- Comparisons and example in speech processing are demonstrated to show that, compared with the STFT and the WVD, the LPFT is a better tool to deal with signals having time-varying frequencies.

Outline

- Work on time-frequency representation (TFR)
  - Introduction
  - Local polynomial Fourier transform (LPFT)
    - Definition
    - Uncertainty principles of second-order and higher-order LPFT
    - Reassignment method for second-order and higher-order LPP
- Work on compressive sensing
- Work on compressive sensing based TFR
- Future work

LPP: local polynomial periodogram

Reassignment method definition

- The reassignment method was applied to the TFR [F. Auger & P. Flandrin, IEEESP, 1995.]

$$RTFR(x;t',\omega') = \int\int TFR(x;t,\omega)\delta(t' - \hat{t}(x;t,\omega))\delta(\omega' - \hat{\omega}(x;t,\omega))dtd\omega$$

- It changes the attribution point of the average operation to the gravitational center of the energy contribution, and the operators are defined as:

$$\hat{t}(x;t,\omega) = t - \frac{\int\int u\phi(u,\Omega)WVD(x;t-u,\omega-\Omega)dud\Omega}{\int\int \phi(u,\Omega)WVD(x;t-u,\omega-\Omega)dud\Omega}$$

$$\hat{\omega}(x;t,\omega) = \omega - \frac{\int\int \Omega\phi(u,\Omega)WVD(x;t-u,\omega-\Omega)dud\Omega}{\int\int \phi(u,\Omega)WVD(x;t-u,\omega-\Omega)dud\Omega}$$

Reassigned Spectrogram

- The gravitational center of the reassigned spectrogram was reported to be

$$\hat{t}(x;t,\omega)=t-\frac{\iint uWVD(h;u,\Omega)WVD(x;t-u,\omega-\Omega)\,du\,d\Omega}{\iint WVD(h;u,\Omega)WVD(x;t-u,\omega-\Omega)\,du\,d\Omega}$$

$$=t-\mathrm{Re}\left\{\frac{STFT_{Th}(x;t,\omega)}{STFT_{h}(x;t,\omega)}\right\}$$

$$\hat{\omega}(x;t,\omega)=\omega-\frac{\iint \Omega WVD(h;u,\Omega)WVD(x;t-u,\omega-\Omega)\,du\,d\Omega}{\iint WVD(h;u,\Omega)WVD(x;t-u,\omega-\Omega)\,du\,d\Omega}$$

$$=\omega+\mathrm{Im}\left\{\frac{STFT_{Dh}(x;t,\omega)}{STFT_{h}(x;t\omega)}\right\}$$

THE REASSIGNED LPP

- Similarly, we define the gravitational center of the reassigned LPP as

$$\hat{t}(x;t,\omega)=t-\frac{\iint uWVD(h;u,-\frac{\omega_1}{2}u+\Omega)WVD(x;t-u,\omega-\frac{\omega_1}{2}u-\Omega)dud\Omega}{\iint WVD(h;u,-\frac{\omega_1}{2}u+\Omega)WVD(x;t-u,\omega-\frac{\omega_1}{2}u-\Omega)dud\Omega}$$

$$=t-\mathrm{Re}\left\{\frac{LPFT_{Th}(x;t,\omega)}{LPFT_h(x;t,\omega)}\right\}$$

$$\hat{\omega}(x;t,\omega)=\omega-\frac{\iint(\Omega-\frac{\omega_1}{2}u)WVD(h;u,-\frac{\omega_1}{2}u+\Omega)WVD(x;t-u,\omega-\frac{\omega_1}{2}u-\Omega)dud\Omega}{\iint WVD(h;u,-\frac{\omega_1}{2}u+\Omega)WVD(x;t-u,\omega-\frac{\omega_1}{2}u-\Omega)dud\Omega}$$

$$=\omega+\mathrm{Im}\left\{\frac{LPFT_{Dh}(x;t,\omega)}{LPFT_h(x;t\omega)}\right\}$$

- Therefore the RLPP is defined as

$$RLPP(x,t,\omega)=\iint LPP(x;t,\omega)\delta(t'-\hat{t}(x;t,\omega))\delta(\omega'-\hat{\omega}(x;t,\omega))dtd\omega$$

Properties of the RLPP

- Non-negativity
- Non-bilinearity
- Time and frequency shifts invariance
- Time-scaling property
- Energy conservation
- Perfect localization on chirp and impulse signals
  - For a chirp signal $x(t) = Ae^{j(\omega_0 t + \alpha t^2/2)}$, we have

    $$RLPP(x;t',\omega') = \int\int LPP(x;t,\omega)\delta(\omega' - \omega_0 - \alpha t)\delta(t' - \hat{t}(x;t,\omega))dtd\omega$$

  - For an impulse signal $x(t) = A\delta(t - t_0)$, we have

    $$RLPP(x;t',\omega') = \delta(t' - t_0)\int\int LPP(x;t,\omega)\delta(\omega' - \hat{\omega}(x;t,\omega))dtd\omega$$

Simulations

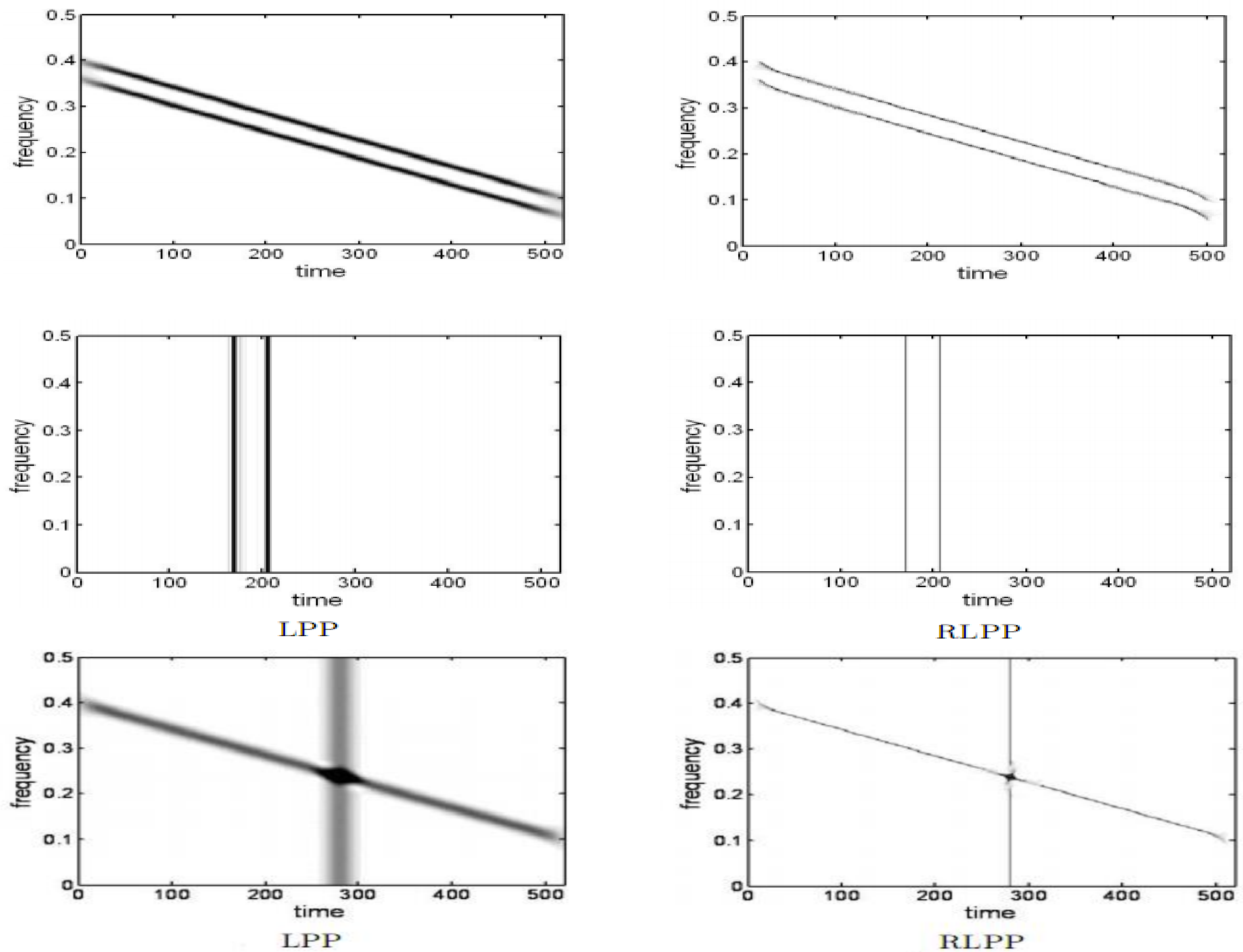

- RLPP can concentrate the chirp signals and impulse signals

SIMULATIONS, CONT'D

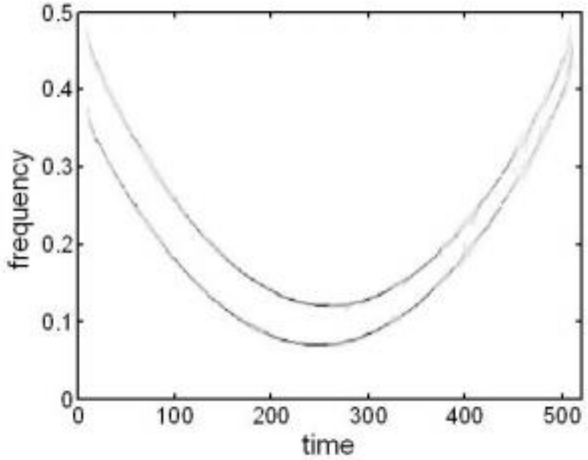

RLPP

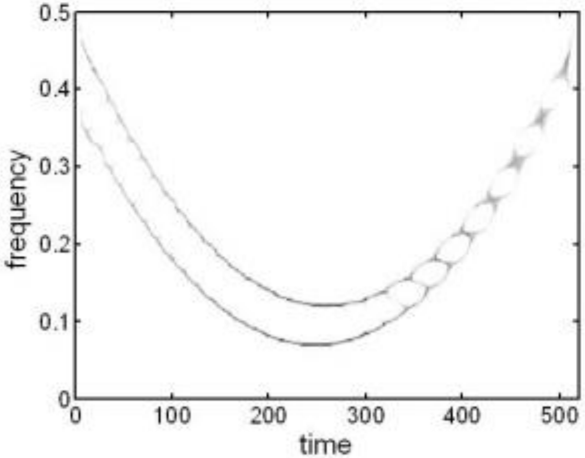

RSP

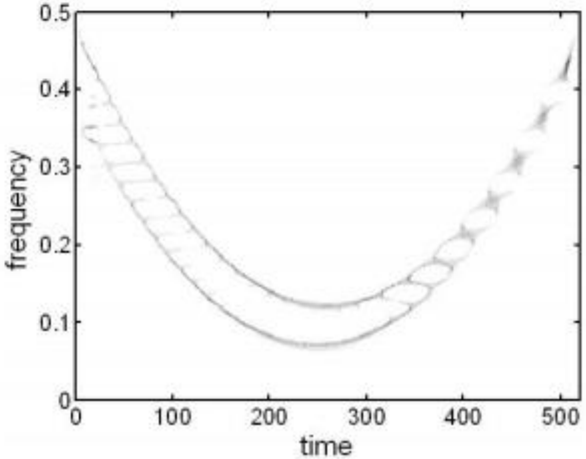

RSPWVD

SIMULATIONS, CONT'D

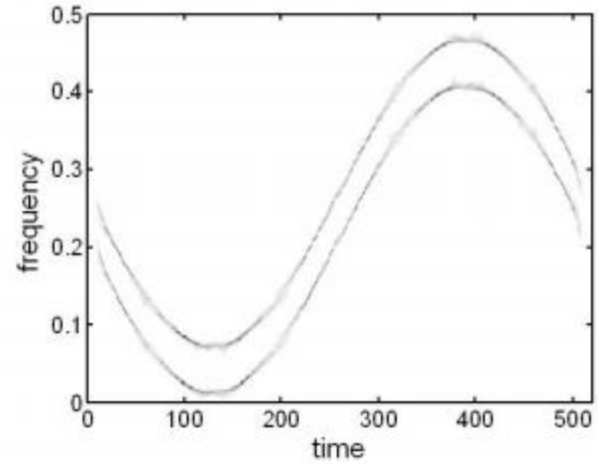

RLPP

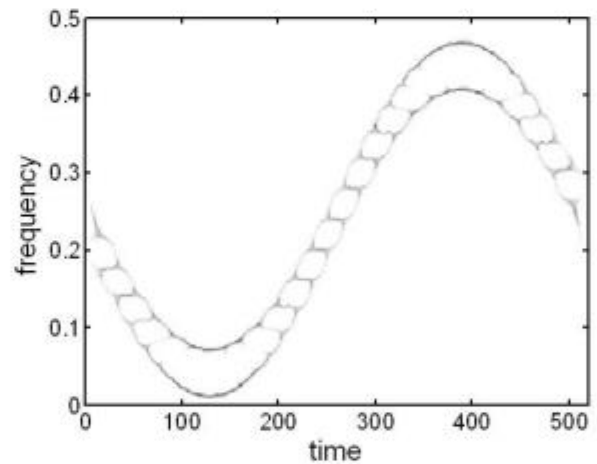

RSP

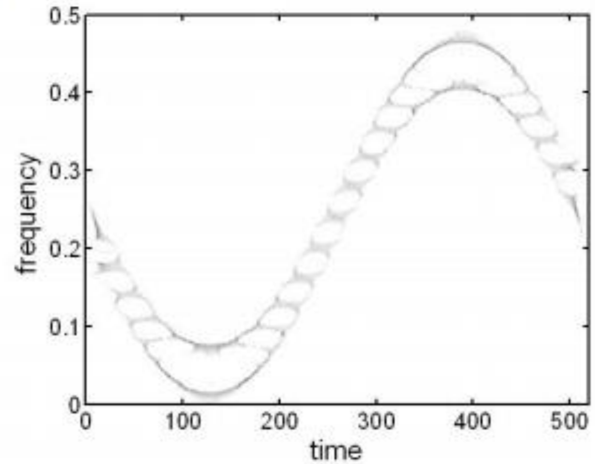

RSPWVD

DEFINITION OF THE HIGHER-ORDER RLPP

- To define the higher order reassigned LPP and its properties, the modified WVD and its properties are first investigated. Based on the modified WVD, the definition of the Mth order reassigned LPP is given.

For the Mth order PPSs, suppose $\phi(t)$ is the phase of the signal, and $\phi^{(m)}(t)$ is the mth-order derivative of Φ. When $M > 4$ and M is odd, the modified WVD is defined as

$$MWVD^{\{M\}}(x;t,\omega) = \int x(t+\frac{\tau}{2})x^*(t-\frac{\tau}{2})e^{-j\omega\tau}$$
$$\cdot e^{-j\frac{\phi^{(3)}\tau^3}{2^2 3!}}e^{-j\frac{\phi^{(5)}\tau^5}{2^4 5!}}...e^{-j\frac{\phi^{(M)}\tau^M}{2^{M-1}M!}}d\tau$$
$$= \int x(t+\frac{\tau}{2})x^*(t-\frac{\tau}{2})e^{-j\omega\tau}e^{-j\sum_{m=3}^{M}\frac{\phi^{(m)}\tau^m}{2^{m-1}m!}}d\tau,$$

when $M \geq 4$ and M is even, the modified WVD is defined

$$MWVD^{\{M\}}(x;t,\omega) = \int x(t+\frac{\tau}{2})x^*(t-\frac{\tau}{2})e^{-j\omega\tau}$$
$$e^{-j\frac{\phi^{(3)}\tau^3}{2^2 3!}}e^{-j\frac{\phi^{(5)}\tau^5}{2^4 5!}}...e^{-j\frac{\phi^{(M-1)}\tau^{M-1}}{2^{M-2}(M-1)!}}d\tau$$
$$= \int x(t+\frac{\tau}{2})x^*(t-\frac{\tau}{2})e^{-j\omega\tau}e^{-j\sum_{m=4}^{M}\frac{\phi^{(m-1)}\tau^{m-1}}{2^{m-2}(m-1)!}}d\tau.$$

Definition of the Higher-order RLPP, Cont'd

$$\hat{t}(x;t,\omega) = t - \frac{\int\int u\, WVD\,(h;u,\Omega)\, MWVD^{\{M\}}\left(x; t-u, \omega + \sum_{m=2}^{M} \frac{(-1)^{m-1}\omega_{m-1}u^{m-1}}{(m-1)!} - \Omega\right)\frac{du d\Omega}{2\pi}}{\int\int WVD\,(h;u,\Omega)\, MWVD^{\{M\}}\left(x; t-u, \omega + \sum_{m=2}^{M} \frac{(-1)^{m-1}\omega_{m-1}u^{m-1}}{(m-1)!} - \Omega\right)\frac{du d\Omega}{2\pi}}$$

$$= t - Re\left\{\frac{LPFT_{Th}^{\{M\}}(x;t,\omega)\; LPFT_{h}^{\{M\}*}(x;t,\omega)}{|LPFT_{h}^{\{M\}}(x;t,\omega)|^2}\right\}$$

$$= t - Re\left\{\frac{LPFT_{Th}^{\{M\}}(x;t,\omega)}{LPFT_{h}^{\{M\}}(x;t,\omega)}\right\},$$

$$\hat{\omega}(x;t,\omega) = \omega - \frac{\int\int \Omega\, WVD\,(h;u,\Omega)\, MWVD^{\{M\}}\left(x; t-u, \omega + \sum_{m=2}^{M} \frac{(-1)^{m-1}\omega_{m-1}u^{m-1}}{(m-1)!} - \Omega\right)\frac{du d\Omega}{2\pi}}{\int\int WVD\,(h;u,\Omega)\, MWVD^{\{M\}}\left(x; t-u, \omega + \sum_{m=2}^{M} \frac{(-1)^{m-1}\omega_{m-1}u^{m-1}}{(m-1)!} - \Omega\right)\frac{du d\Omega}{2\pi}}$$

$$= \omega + Im\left\{\frac{LPFT_{Dh}^{\{M\}}(x;t,\omega)\; LPFT_{h}^{\{M\}*}(x;t,\omega)}{|LPFT_{h}^{\{M\}}(x;t,\omega)|^2}\right\}$$

$$= \omega + Im\left\{\frac{LPFT_{Dh}^{\{M\}}(x;t,\omega)}{LPFT_{h}^{\{M\}}(x;t,\omega)}\right\}.$$

$$RLPP^{\{M\}}(x;t',\omega') = \int\int LPP^{\{M\}}(x;t,\omega)\,\delta\left[\omega' - \hat{\omega}(x;t,\omega)\right]\delta\left[t' - \hat{t}(x;t,\omega)\right] dt\frac{d\omega}{2\pi}.$$

Properties of higher-order RLPP

- time and frequency shifts invariance

  for a signal $y(t) = x(t - t_0)e^{j\omega_0 t}$, we have

$$RLPP^{\{M\}}(y;t',\omega') = RLPP^{\{M\}}(x;t'-t_0,\omega'-a_1).$$

- time-scaling property

  for a signal $y(t) = x(at)$, we have

$$RLPP^{\{M\}}(y;t',\omega') = \frac{1}{|a|}RLPP^{\{M\}}(x;at',\frac{\omega'}{a}).$$

- energy conservation

$$\int\int RLPP^{\{M\}}(x;t',\omega')\frac{dt'd\omega'}{2\pi} = \int |x(t)|^2 dt,$$

when

$$\int\int WVD(h;u,\Omega)\frac{dud\Omega}{2\pi} = 1.$$

Properties of higher-order RLPP, Cont'd

- perfect localization on higher-order PPSs

For other higher-order PPSs such as $x(t) = A\exp\{j\sum_{m=0}^{M}\frac{a_m t^m}{m!}\}$, we have

$$MWVD^{\{M\}}(x;t,\omega) = 2\pi A^2\delta(\omega - a_1 - a_2 t - \frac{a_3 t^2}{2!} - \ldots \frac{a_M t^{M-1}}{(M-1)!}),$$

therefore, the corresponding reassigned LPP with the same order can also perfectly localize the PPSs as

$$RLPP^{\{M\}}(x;t',\omega') = \int\int LPP^{\{M\}}(x;t,\omega)$$
$$\cdot\delta(\omega' - a_1 - a_2 t - \frac{a_3 t^2}{2!} - \ldots \frac{a_M t^{M-1}}{(M-1)!})$$
$$\cdot\delta\left[t' - \hat{t}(x;t,\omega)\right] dt\frac{d\omega}{2\pi}.$$

Simulations, Cont'd

- Fourth-order

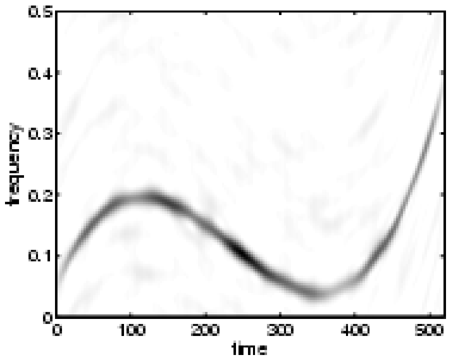

(a) LPP

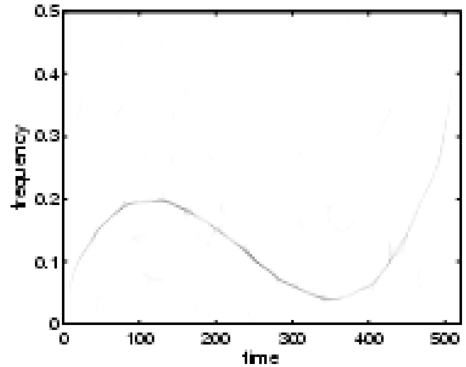

(b) RLPP

- Fifth-order

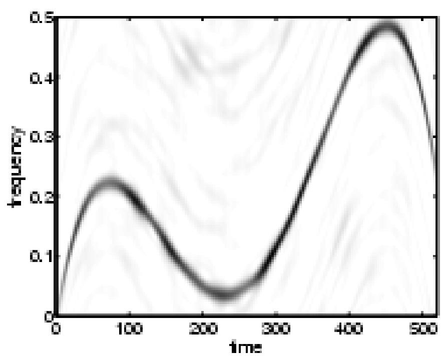

(d) LPP

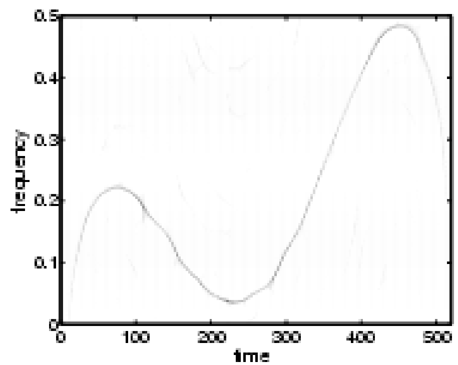

(e) RLPP

Simulations, Cont'd

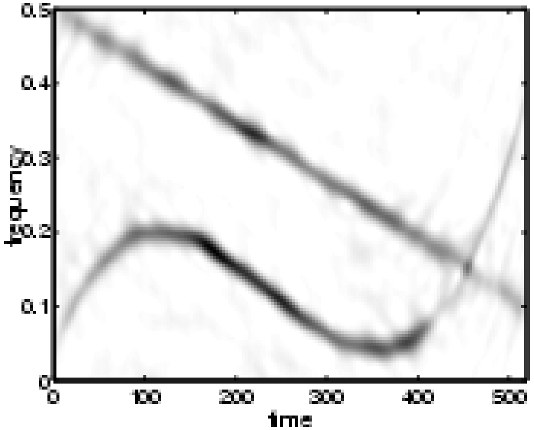

(a) LPP

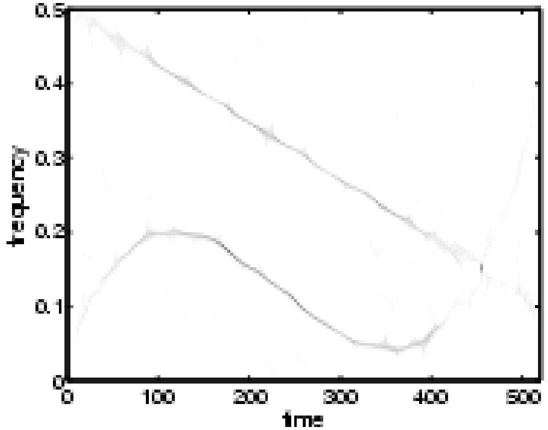

(b) RLPP

The LPP, RLPP for a signal containing
two PPSs of second and fourth orders, respectively,
with SNR $= 0$dB.

Summary of reassignment methods of LPFT

- The reassignment method is extended to the second-order LPP and higher-order LPP to improve the signal concentration performance for time-varying signals.
- Properties of the second-order RLPP and higher-order RLPP are studied and theoretically derived.
- Simulation results are also presented to verify some properties and improvements of the second-order RLPP. Moreover, performances of the higher-order RLPP for higher-order PPSs are presented to show the advantage of the higher-order RLPP.

Outline

- Work on time-frequency representation (TFR)
- Work on compressive sensing
  - Introduction on compressive sensing
  - Compressive sensing based image reconstruction
- Work on compressive sensing based TFR
- Future work

Introduction on compressive sensing

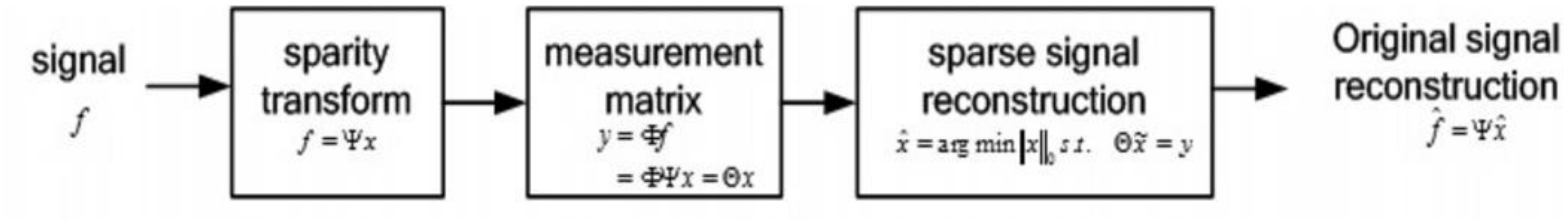

Fig. 1. The diagram of compressive sensing

Compressive sensing based image reconstruction

- When using the traditional compressive sensing algorithm for image reconstruction, the wavelet decomposition divides the image into high-frequency coefficients and low-frequency coefficients, most high-frequency coefficients are around zero and therefore can be considered as sparse.

COMPRESSIVE SENSING BASED IMAGE RECONSTRUCTION

- However, the low-frequency coefficients cannot be considered as sparse since they concentrate most of the image energy and they are the approximation of the original image.
- Therefore, when using the traditional compressive sensing algorithm by putting the low-frequency coefficients together with the high-frequency coefficients to multiply with the measurement matrix, the coherences among the low-frequency coefficients will be disrupted, and the reconstructed image will have a degraded performance.

Compressive sensing based image reconstruction : Our work

- After the wavelet transform of the image, we keep the low-frequency coefficients unchanged, use the measurement matrix to measure the high-frequency coefficients, and then combine with the unchanged low-frequency coefficients to reconstruct the image.
- In this way, we can efficiently reconstruct the image with reduced coefficients as well as improve the performance of the reconstructed images.
- we also will give the performance comparisons of the reconstructed images employing different measurement matrices such as the Gaussian random matrix, Bernoulli matrix, Toeplitz matrix, and Hadamard matrix

Image reconstruction based on the improved compressive sensing algorithm

(1) Perform the wavelet transform of the N*N image, and get the four wavelet sub-band coefficients $\{LH_1, HL_1, HH_1, LL_1\}$.

(2) build the measurement matrix to measure the three high-frequency sub-band coefficients LH_1, HL_1, HH_1 to get the matrices of the measured coefficients while keep the low-frequency sub-band coefficients LL_1 unchanged.

(3) Use the reconstruction algorithms to reconstruct the three high-frequency coefficients matrices $\overline{LH_1}, \overline{HL_1}, \overline{HH_1}$, then together with LL_1, to reconstruct the image.

Simulations and Comparisons

- **Performance comparisons of the reconstructed images using traditional and improved CS algorithms**

(a) Original image

(b) image reconstructed using the traditional CS algorithm, M=190.

(c) image reconstructed using the traditional CS algorithm, M=100

(d) image reconstructed using the improved CS algorithm, M=100.

Figure 2. The original image and the reconstructed images using the traditional and improved CS algorithm

using the traditional CS algorithm to reconstruct the image: perform the 4-layer decomposition for the image, Gaussian random matrix as the measurement matrix, and the OMP algorithm.

Fig. 2(b), M=190, PSNR=30.8075dB.
Fig. 2 (c), M=100, PSNR=23.9248dB.

using the improved compressive sensing algorithm for image reconstruction: perform the single-layer wavelet decomposition

Fig. 2 (d), M=100, PSNR= 30.0757 dB.

Simulations and Comparisons

- performances of the reconstructed images using the traditional and improved compressive sensing algorithms with different M values

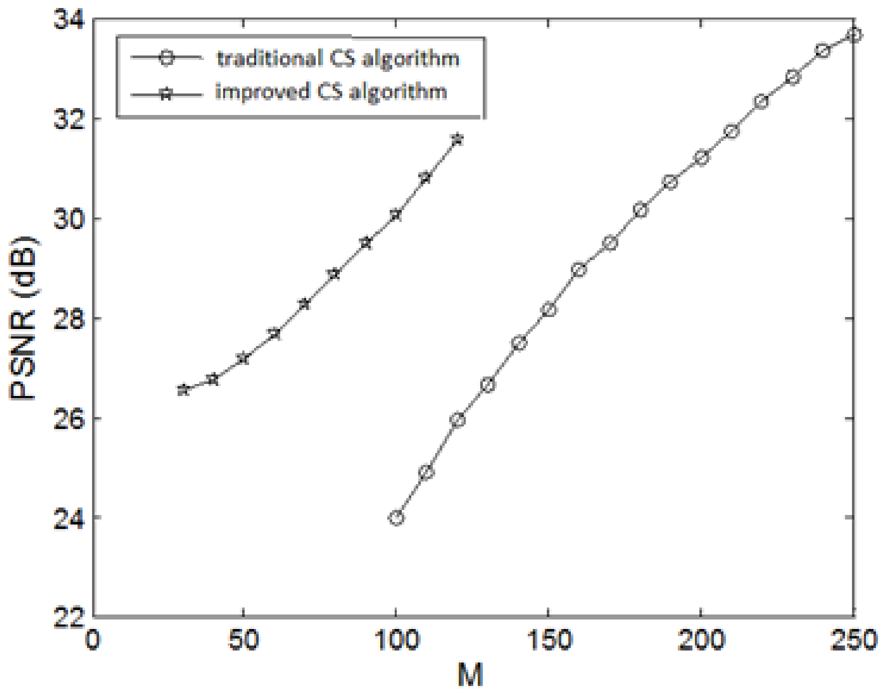

Figure 3. Performance comparisons between the traditional CS algorithm and improved CS algorithm in different M values.

with the same measurement numbers, the improved CS algorithm can effectively improve the PSNR of the reconstructed image.

Simulations and Comparisons

- **Performance comparisons of the reconstructed images using different measurement matrices:** Gaussian random matrix, Bernoulli matrix, Toeplitz matrix, and Hadamard matrix.

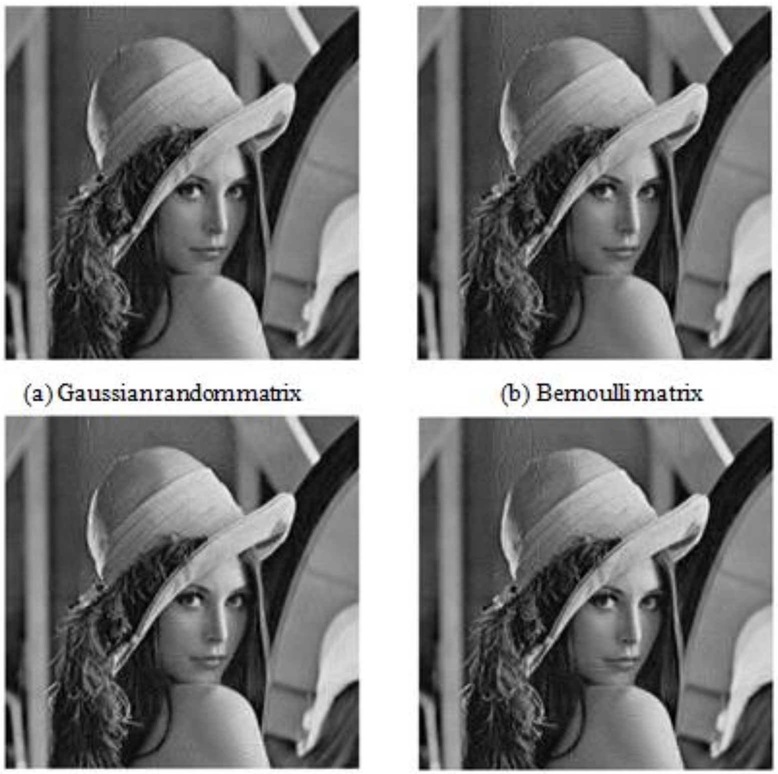

(a) Gaussianrandommatrix (b) Bernoulli matrix (c) Toeplitz matrix (d) Hadamardmatrix

Figure 4. Using different matrices for image reconstruction in the improved CS algorithm with M=50.

M=50, the four measurement matrices can achieve comparable reconstructed performances with similar PSNR.

Table I PSNR comparisons using different matrices for image reconstruction in the improved CS algorithm with M=50.

Measurement matrix	PSNR of the reconstructed image (dB)
Gaussian random matrix	27.1996
Bernoulli matrix	27.0512
Toeplitz matrix	27.1089
Hadamard matrix	27.2567

Simulations and Comparisons

(a) Gaussianrandommatrix (b) Bernoulli matrix (c) Toeplitz matrix (d) Hadamard matrix

Figure 5. Using different matrices for image reconstruction in the improved CS algorithm with M=100.

M=100, the reconstructed image using the Hadamard matrix can achieve better performance with higher PSNR.

Table II PSNR comparisons using different matrices for image reconstruction in the improved CS algorithm with M=100.

Measurement matrix	**PSNR of the reconstructed image (dB)**
Gaussian random matrix	30.0455
Bernoulli matrix	30.1990
Toeplitz matrix	30.1518
Hadamard matrix	32.2892

Simulations and Comparisons

- to investigate the effects of the four measurement matrices to the reconstructed images in different M values, we provide the PSNRs of the reconstructed images using different M=[30:120],

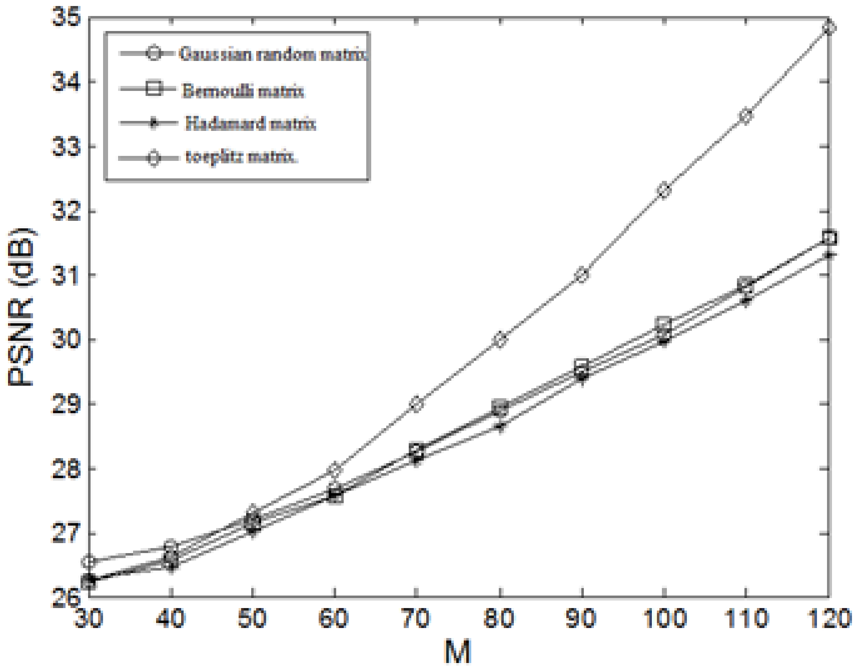

Figure 6 Performance comparisons of the reconstructed images using the improved CS algorithm with different measurement matrices.

As the M increases, higher PSNR can be achieved when using the Hadamard matrix as the measurement matrix.

Summary on Compressive sensing based image reconstruction

- Based on the improved CS algorithm, we only measure the high-frequency wavelet coefficients, and combines with the unchanged low-frequency coefficients to reconstruct the image.

- Compared with the traditional CS algorithm with the same measurement numbers, the improved CS algorithm can effectively improve the performance of the reconstructed images.

- Reconstructed image performance comparisons are given for different measurement matrices such as Gaussian random matrix, Bernoulli matrix, Toeplitz matrix, and Hadamard matrix. Better reconstructed image performance can be achieved with higher PSNR when using Hadamard matrix as the measurement matrix.

OUTLINE

- Work on time-frequency representation (TFR)
- Work on compressive sensing
  - Introduction on compressive sensing
    - Introduction
    - Compressive sensing based image reconstruction
- Work on compressive sensing based TFR
- Future work

COMPRESSIVE SENSING BASED TFR

Suppose the analyzed nonstationary signal is of length N in time, and after the time-frequency analysis, its time-frequency representation is of $N \times N$ when computed over N frequency bins. Since the energy of the nonstationary signal is concentrated in a certain trajectory, and at most only N values are expected to be non-zero. Therefore the nonstationary signal is sparse or compressible in the time-frequency domain, and satisfies the sparse condition in the compressive sensing.

COMPRESSIVE SENSING BASED TFR

- E. Candes proved that it is possible to reconstruct the signal from its partial Fourier coefficients. [E. Candes, IEEEIT, 2006]

- Since the ambiguity function (AF) is related to the WVD by a two-dimensional Fourier transform, we can use the samples in the AF domain to reconstruct the time frequency representation. [P. Flandrin, IEEESP, 2010]

COMPRESSIVE SENSING BASED TFR

The ambiguity function (AF) is important in the field of time frequency analysis, and its definition for a signal $f(t)$ is as follows:

$$A(f;\theta,\tau) = \int_{-\infty}^{\infty} f(t+\frac{\tau}{2})f^{*}(t-\frac{\tau}{2})e^{j\theta t}dt. \tag{4}$$

In the AF domain, the auto terms pass through the origin of the TF plane, while the cross terms are away from the origin.

COMPRESSIVE SENSING BASED TFR

The algorithm to reconstruct the time-frequency representations based on the compressive sensing includes the following steps:

1. compute the ambiguity function of the nonstationary signals;

2. using window function, such as the rectangular window function or the Gaussian window function, to select the few samples in the origin part of the AF domain, which mainly includes the auto terms;

3. using the reconstruction algorithm in the compressive sensing to reconstruct the time-frequency representation of the nonstationary signals from the few samples in the origin part of the AF domain.

COMPRESSIVE SENSING BASED TFR : SIMULATIONS AND COMPARISONS

monocomponent signal

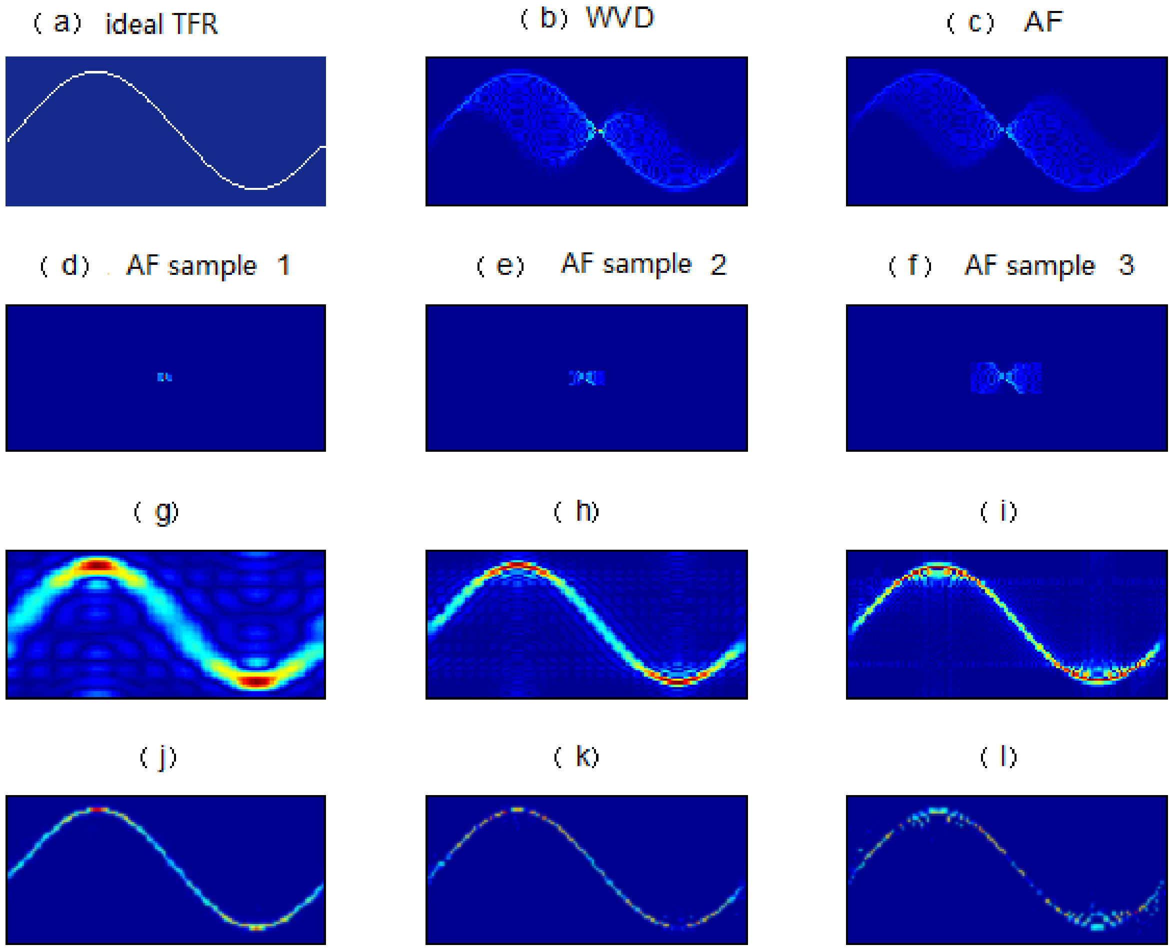

(g)-(i): TFR reconstruction based on the direct Fourier transform
(j)-(l): TFR reconstruction based on the compressive sensing

COMPRESSIVE SENSING BASED TFR : SIMULATIONS AND COMPARISONS

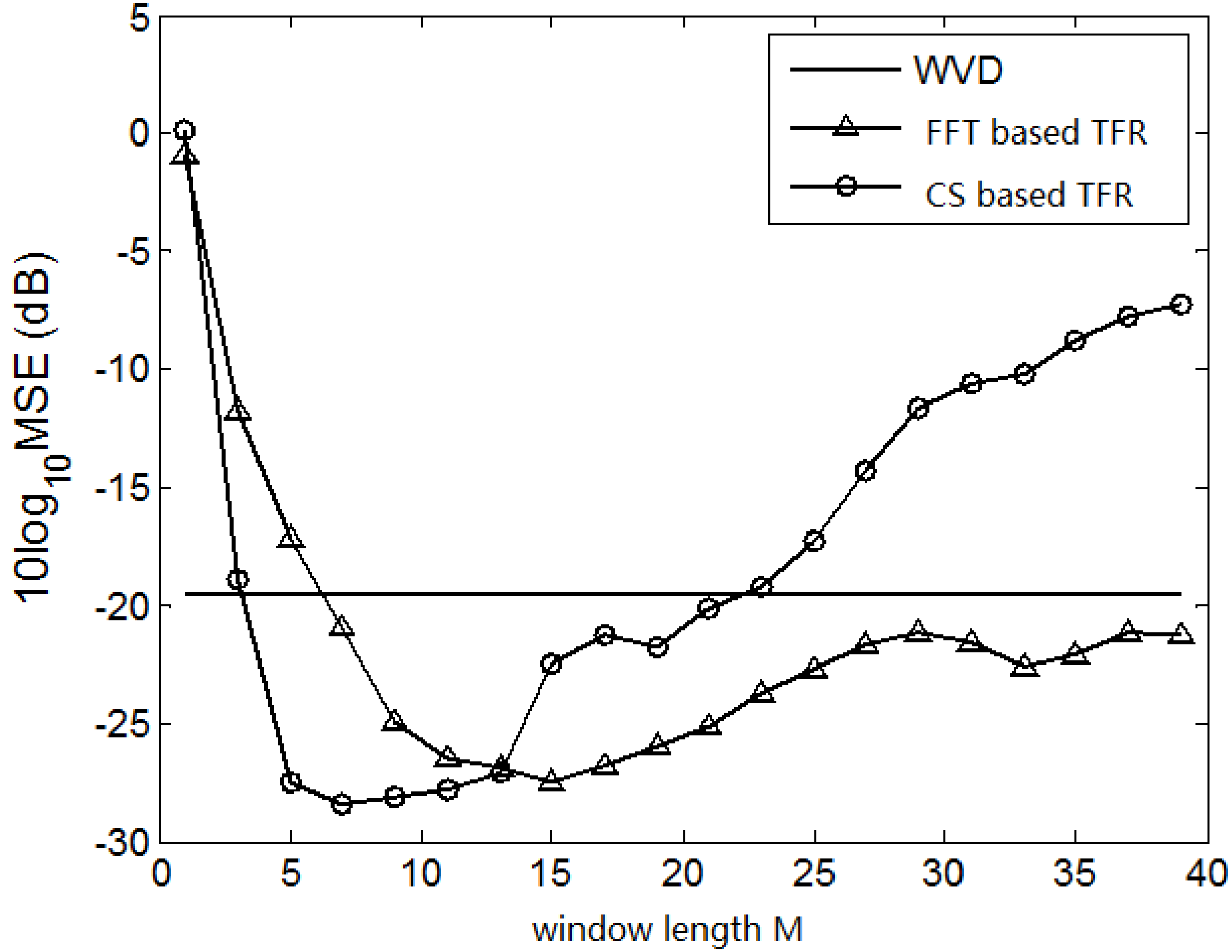

IF estimation MSE of monocomponent signal TFR reconstruction

COMPRESSIVE SENSING BASED TFR : SIMULATIONS AND COMPARISONS

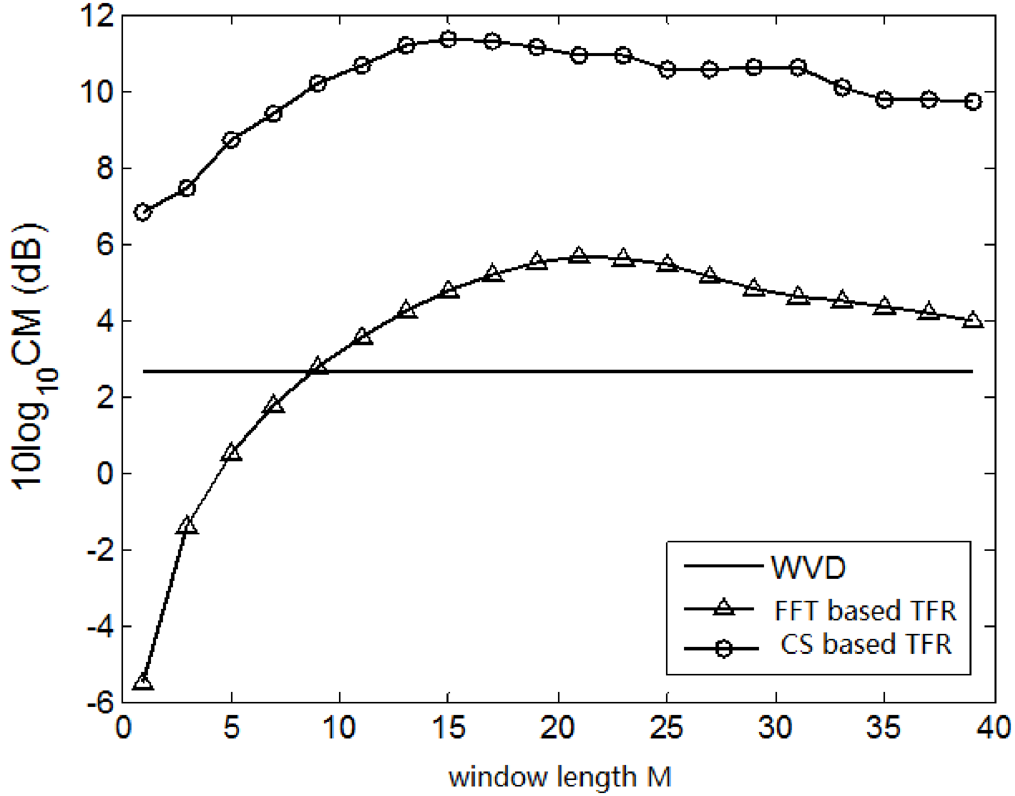

Concentration measurement of monocomponent signal TFR reconstruction

When the window length is between [5,21], the CS based TFR can achieve smaller IF estimation errors and higher time-frequency concentration, compared with the FFT based TFR

COMPRESSIVE SENSING BASED TFR : SIMULATIONS AND COMPARISONS

multicomponent signal

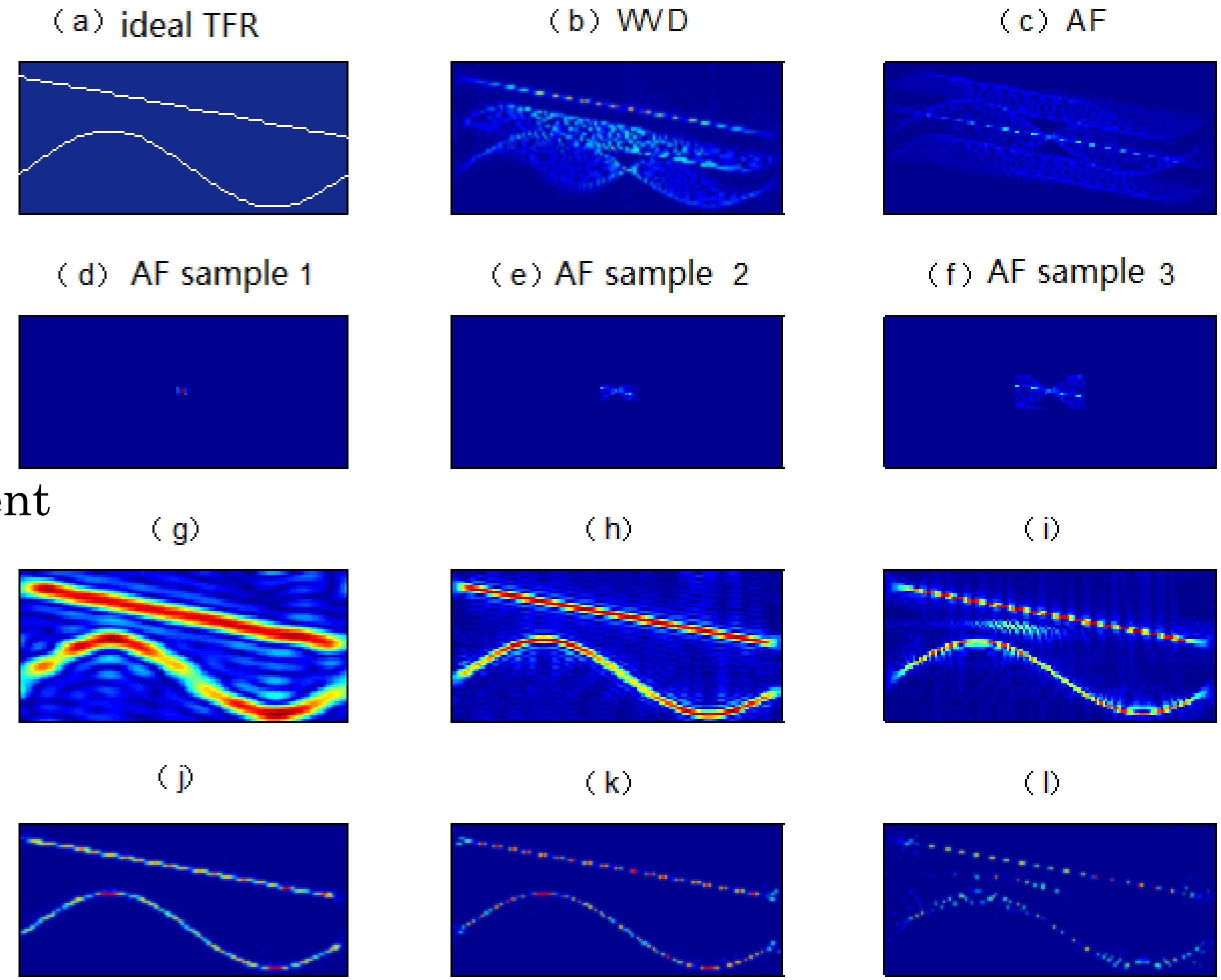

(g)-(i): TFR reconstruction based on the direct Fourier transform

(j)-(l): TFR reconstruction based on the compressive sensing

COMPRESSIVE SENSING BASED TFR : SIMULATIONS AND COMPARISONS

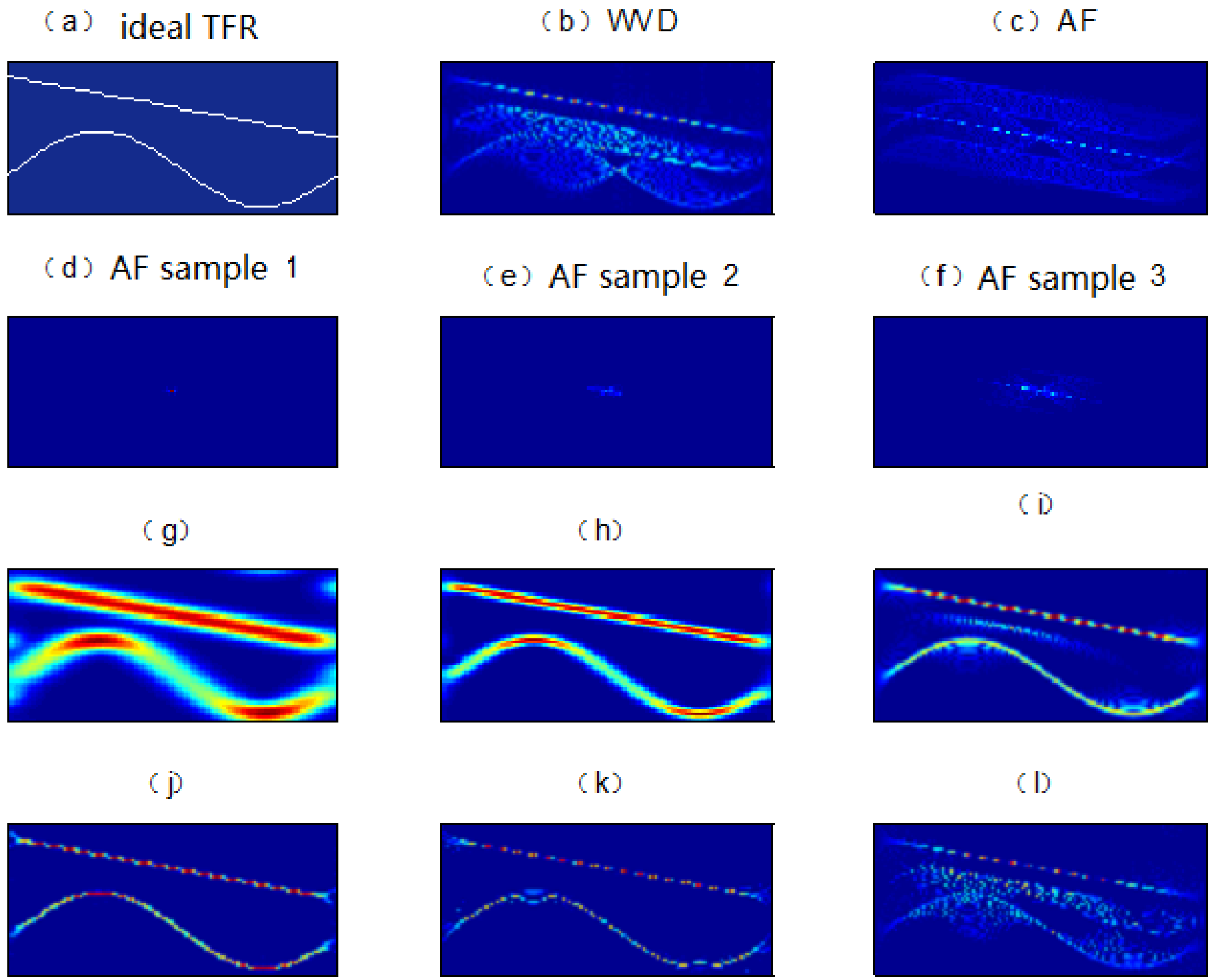

Gaussian window, multicomponent signal

COMPRESSIVE SENSING BASED TFR : SIMULATIONS AND COMPARISONS

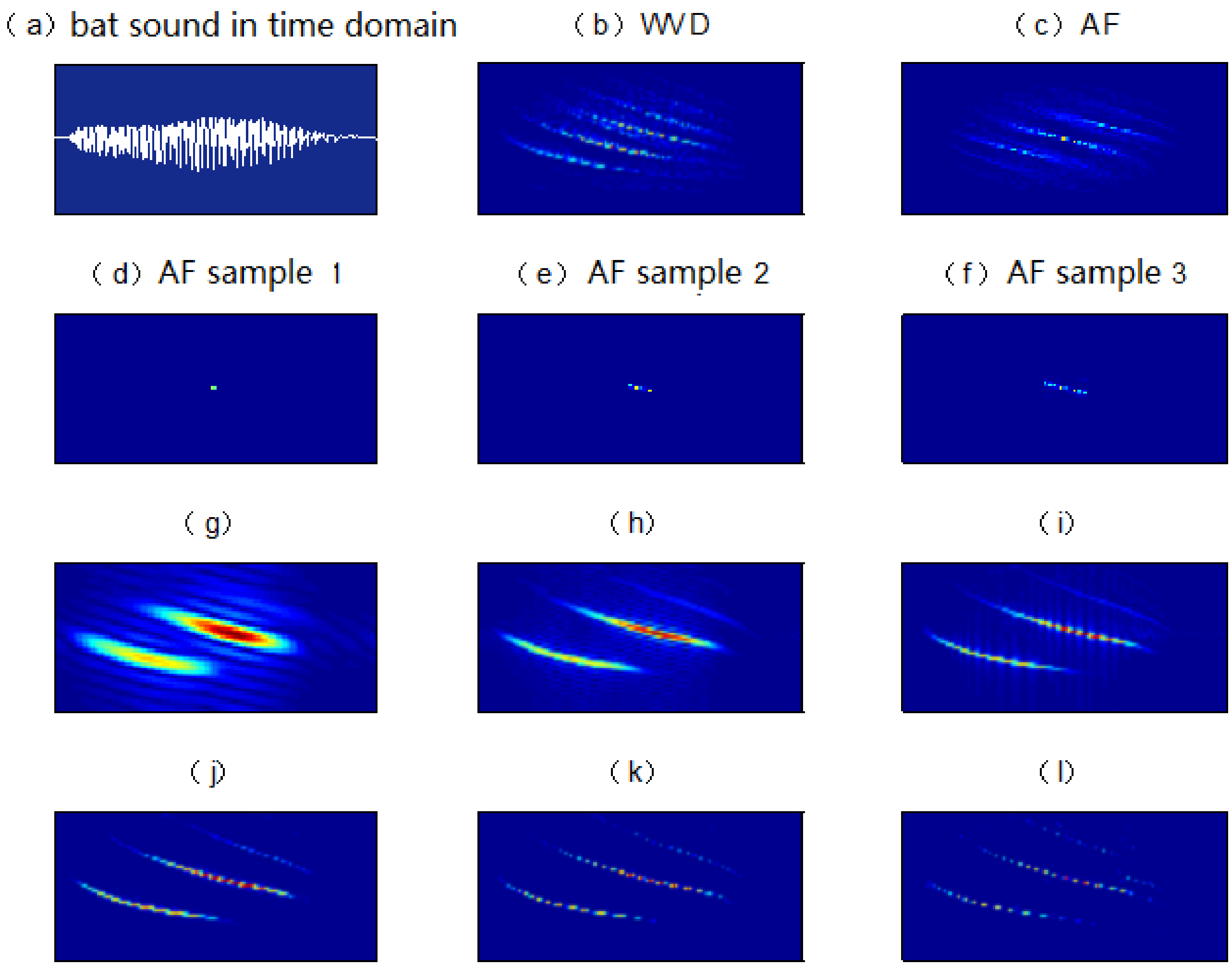

(g)-(i): bat sound TFR reconstruction based on the direct Fourier transform

(j)-(l): bat sound TFR reconstruction based on the compressive sensing

Summary on compressive sensing based TFR

- The compressive sensing is employed to reconstruct the time-frequency representation of the nonstationary signals.
- Using window function to select the auto terms concentrated on the origin of the AF domain, followed by the reconstruction algorithm, the time-frequency representation of the signals can be reconstructed.
- Performances of different window sizes are discussed and compared, showing that there exists a tradeoff between the resolution and the cross terms in the reconstructed representations.

Outline

- Work on time-frequency representation (TFR)
- Work on compressive sensing
- Work on compressive sensing based TFR
- Future work

Future work

- how to reconstruct the time-frequency representations for the signals, taking advantage of the structured sparseness of the signals? (sparse Bayesian learning)
- how to select the proper sample region to reconstruct the time-frequency representation for signals? (signal-dependent)
- how to reconstruct the time-frequency representations for the signals heavily corrupted by noise such as white Gaussian noise or impulsive noise?

Thanks !